Nucleon Sigma Terms with $N_f = 2 + 1$ Flavors of $\mathcal{O}(a)$-Improved Wilson Fermions

A. Agadjanov,[1] D. Djukanovic,[2,3] G. von Hippel,[1] H. B. Meyer,[1,2] K. Ottnad,[1] and H. Wittig[1,2]
[1]*PRISMA$^+$ Cluster of Excellence and Institut für Kernphysik, Johannes Gutenberg-Universität Mainz, D-55099 Mainz, Germany*
[2]*Helmholtz Institute Mainz, Staudingerweg 18, D-55128 Mainz, Germany*
[3]*GSI Helmholtzzentrum für Schwerionenforschung, D-64291 Darmstadt, Germany*

(Received 22 March 2023; revised 16 October 2023; accepted 16 November 2023; published 27 December 2023)

We present a lattice-QCD based analysis of the nucleon sigma terms using gauge ensembles with $N_f = 2 + 1$ flavors of $\mathcal{O}(a)$-improved Wilson fermions, with a complete error budget concerning excited-state contaminations, the chiral interpolation as well as finite-size and lattice spacing effects. We compute the sigma terms determined directly from the matrix elements of the scalar currents. The chiral interpolation is based on SU(3) baryon chiral perturbation theory using the extended on-mass shell renormalization scheme. For the pion nucleon sigma term, we obtain $\sigma_{\pi N} = (43.7 \pm 3.6)$ MeV, where the error includes our estimate of the aforementioned systematics. The tension with extractions based on dispersion theory persists at the 2.4-σ level. For the strange sigma term, we obtain a nonzero value, $\sigma_s = (28.6 \pm 9.3)$ MeV.

DOI: 10.1103/PhysRevLett.131.261902

Introduction.—The scalar matrix element of the nucleon is an important observable, and plays a crucial role in interpreting the results of dark-matter direct-detection experiments. Especially appealing candidates for cold dark matter are weakly interacting massive particles (WIMP), as they naturally reproduce the observed relic abundance of dark matter through annihilation processes in the early Universe. In particular for Higgs-portal models, in which the WIMP-nucleus interaction is mediated by the Higgs boson, the spin-independent cross section for WIMP-nucleus recoil experiments is sensitive to the values of the scalar matrix element [1]. The light-quark scalar matrix element [2]

$$\sigma_{\pi N} \equiv m_l \langle N|\bar{u}u + \bar{d}d|N\rangle = m_l(\partial m_N/\partial m_l), \qquad (1)$$

where $m_l \equiv (m_u + m_d)/2$, also known as the pion-nucleon sigma term, is of special interest. Phenomenologically, $\sigma_{\pi N}$ is accessible via πN-scattering amplitudes at the Cheng-Dashen point [3]. Historically, the value for $\sigma_{\pi N} \sim 45$ MeV derived in [4] was prevalent for a long time, a value compatible with most lattice determinations. However, new analyses using constraints from pionic hydrogen and deuterium led to a much larger value of $\sigma_{\pi N} = 59.1(3.5)$ MeV [5], consistent with the effective field theory (EFT) analysis of [6] and in agreement with [7] based on low-energy πN scattering (see Ref. [8] for a review). By contrast, lattice calculations for $\sigma_{\pi N}$ [9–20], discussed in detail in the FLAG report [21], have largely confirmed the lower estimate, while being in tension with the latest dispersive analysis at the level of 3–4 standard deviations. See Refs. [22–25] for further efforts to extract $\sigma_{\pi N}$ from collections of lattice data for the light-quark-mass dependence of m_N. Very recently, it was suggested that the discrepancy is alleviated via an explicit treatment of $N\pi$ and $N\pi\pi$ excited states in the analysis [26]. As a related quantity, the strangeness matrix element,

$$\sigma_s \equiv m_s \langle N|\bar{s}s|N\rangle = m_s(\partial m_N/\partial m_s), \qquad (2)$$

a pure sea-quark effect, has often been discussed together with the pion-nucleon sigma term. Their linear combination,

$$\sigma_0 \equiv m_l \langle N|\bar{u}u + \bar{d}d - 2\bar{s}s|N\rangle = \sigma_{\pi N} - (2m_l/m_s)\sigma_s, \qquad (3)$$

is to first order in $(m_l - m_s)$ proportional to the nucleon-hyperon mass splitting. The σ_0 value inferred from this observation, assuming a negligible strangeness content σ_s of the nucleon, corresponds to a small value for $\sigma_{\pi N}$. In [27] however, corrections to σ_0 were calculated which bring the associated $\sigma_{\pi N}$ estimate back into agreement with its Cheng-Dashen-theorem based determinations without the need to invoke a large σ_s value.

We perform a direct determination of the nucleon sigma terms from a lattice calculation of the matrix element of the scalar current. Our final estimates are based on a simultaneous chiral, continuum and infinite volume extrapolation of the pion-nucleon, and strange sigma terms. We average the individual fits with weights based on the Akaike information criterion (AIC) [28,29] to provide a full error

Published by the American Physical Society under the terms of the Creative Commons Attribution 4.0 International license. Further distribution of this work must maintain attribution to the author(s) and the published article's title, journal citation, and DOI. Funded by SCOAP^3.

TABLE I. Details of CLS ensembles used in this Letter. The pion and kaon masses are taken from [34] and the lattice spacings from [35]. Using Eq. (16) the largest source-sink separations correspond to 1.4 fm and 1.5 fm for the two finer and coarser lattices, respectively.

ID	t_0/a^2	M_π (MeV)	M_K (MeV)	$M_\pi L$	$\{t_s^{\min}, t_s^{\max}, t_s^{\text{step}}\}/a$
H102	2.860	352	437	4.93	{4,17,1}
N101	2.860	278	461	5.83	{4,17,1}
H105	2.860	277	462	3.88	{4,17,1}
C101	2.860	219	470	4.59	{4,17,1}
S400	3.659	349	440	4.32	{4,22,2}
N451	3.659	286	461	5.31	{4,20,2}
D450	3.659	215	475	5.33	{4,20,1}
D452	3.659	154	482	3.80	{4,20,2}
N203	5.164	346	442	5.40	{4,24,2}
S201	5.164	288	467	3.00	{4,22,2}
N200	5.164	284	463	4.43	{4,22,2}
D200	5.164	200	480	4.16	{4,22,2}
E250	5.164	128	489	4.00	{4,22,2}
N302	8.595	344	450	4.17	{4,28,2}
J303	8.595	257	474	4.14	{4,28,2}
E300	8.595	174	490	4.22	{4,28,2}

budget accounting for variations in the treatment of excited-state contaminations, discretization errors, finite-volume effects, and the quark-mass dependence.

Simulation details.—We employ the $N_f = 2 + 1$ ensembles [30] generated as part of the Coordinated Lattice Simulations (CLS) initiative with nonperturbatively $\mathcal{O}(a)$-improved Wilson fermions [31] and the tree-level improved Lüscher-Weisz gauge action [32], correcting for the treatment of the strange quark determinant using [33]. Table I gives details of the ensembles used in this Letter. In particular, lattice spacings range from 0.050 to 0.086 fm.

The two-point and three-point functions needed to extract the scalar matrix elements of the nucleon read

$$C_2(t;\mathbf{p}) = \Gamma_{\alpha\beta}\sum_{\mathbf{x}} e^{-i\mathbf{p}\mathbf{x}}\left\langle \Psi_\beta(\mathbf{x},t)\bar{\Psi}_\alpha(0)\right\rangle, \tag{4}$$

$$C_3(t,t_s;\mathbf{q}) = \Gamma'_{\alpha\beta}\sum_{\mathbf{x},\mathbf{y}} e^{i\mathbf{q}\mathbf{y}}\left\langle \Psi_\beta(\mathbf{x},t_s)S_q(\mathbf{y},t)\bar{\Psi}_\alpha(0)\right\rangle \tag{5}$$

where S_q denotes the scalar density,

$$S_q = \bar{q}q, \qquad q = u,d,s. \tag{6}$$

The interpolating operator for the proton,

$$\Psi_\alpha(x) = \epsilon_{abc}\left[\tilde{u}_a^T(x)C\gamma_5\tilde{d}_b(x)\right]\tilde{u}_{c,\alpha}(x), \tag{7}$$

is built using Gaussian-smeared quark fields [36]

$$\tilde{q} = (1+\kappa_G\Delta)^{N_G}q, \qquad q = u,d, \tag{8}$$

and spatially APE-smeared gauge links in the covariant Laplacian Δ [37].

The pertinent Wick contractions for the three-point function lead to the connected and disconnected contributions, $C_3 = C_3^{\text{conn}} + C_3^{\text{disc}}$. For the connected part, we employ extended propagators via the "fixed-sink" method, requiring additional inversions for each chosen value of t_s [38]. In order to reduce the cost of the inversions, we apply the truncated solver method with bias correction [39–41]. For the connected part, the polarization matrices Γ', Γ read

$$\Gamma' = \Gamma = \frac{1}{2}(1+\gamma_0)(1+i\gamma_5\gamma_3). \tag{9}$$

The disconnected three-point function is constructed from the quark loop L^q and the nucleon two-point function

$$C_3^{\text{disc}}(t,t_s;\mathbf{q}) = \left\langle e^{-i\mathbf{q}\mathbf{x}}L^q(\mathbf{q},z_0)\cdot C_2(\mathbf{p}',y_0,x;\Gamma')\right\rangle, \tag{10}$$

where

$$L^q(\mathbf{q},z_0) = -\sum_{\mathbf{z}\in\Lambda} e^{i\mathbf{q}\cdot\mathbf{z}}\mathrm{Tr}\left[D_q^{-1}(z;z)\mathbb{1}\right]. \tag{11}$$

Note that for forward scalar matrix elements ($\mathbf{q} = 0$), the vacuum expectation value of the current insertion must be subtracted,

$$\begin{aligned} C_3^{\text{disc}}(t,t_s;\mathbf{0}) = &\left\langle L^q(\mathbf{0},z_0)\cdot C_2(\mathbf{p}',y_0,x;\Gamma')\right\rangle \\ &- \left\langle L^q(\mathbf{0},z_0)\right\rangle\cdot\left\langle C_2(\mathbf{p}',y_0,x;\Gamma')\right\rangle. \end{aligned} \tag{12}$$

Additionally, we improve the signal by averaging over all three different polarizations

$$\Gamma'_i = \frac{1}{2}(1+\gamma_0)(1+i\gamma_5\gamma_i), \qquad i = 1,2,3, \tag{13}$$

and by averaging over forward and backward propagating nucleons. Traces over the quark loops are estimated stochastically using four-dimensional noise vectors η. We improve the precision of the quark loops using a variation of the frequency splitting method [42] that combines the one-end trick [43] with a generalized hopping parameter expansion [44] and hierarchical probing [45] (for more details see Appendix C of Ref. [46]).

Let $G_S \equiv \langle N|S_q|N\rangle$ denote the nucleon scalar form factor at vanishing momentum transfer. It can be extracted from the ratio of correlation functions

$$G_S^{\text{eff}}(t,t_s) \equiv \mathrm{Re}\frac{C_3(t,t_s;\mathbf{0})}{C_2(t_s;\mathbf{0})}. \tag{14}$$

Indeed, let Δ be the energy gap between the lowest excited state and the ground state. Performing the spectral decomposition in Eq. (14) and taking the limit of t, $(t_s - t) \gg \Delta^{-1}$, we obtain

$$G_{\mathrm{S}}^{\mathrm{eff}}(t,t_s) \xrightarrow{t,(t_s-t)\gg\Delta^{-1}} G_{\mathrm{S}}. \tag{15}$$

We extract the ground-state contribution for each flavor combination of the scalar current corresponding to $\sigma_{\pi N}$, σ_s, and σ_0. Errors are computed using the bootstrap method on binned data with a bin size of 2. For the conversion to physical units, we first express dimensionful quantities in units of t_0 using Ref. [35] (see Table I) and finally use the value from [21]

$$\sqrt{t_0} = 0.14464(87)\ \mathrm{fm} \tag{16}$$

to calibrate the scale.

Excited-state analysis.—A major obstacle to achieving reliable and precise determinations of the ground-state matrix element is the well-known noise problem of nucleon correlation functions [47,48]. For typical source-sink separations in current lattice calculations, the ratio in Eq. (14) will be contaminated by exponentially suppressed terms associated with resonances and multihadron states. Several approaches were developed to have a better control over the excited-state systematics (see Refs. [49,50] and references therein). The summation method [51–53] and multistate fits are the most widely used among them.

In the summation method, the ground-state matrix element is determined from the summed ratio

$$S(t_s) = a\sum_{t=a}^{t_s-a} G_{\mathrm{S}}^{\mathrm{eff}}(t,t_s) \xrightarrow{t_s\gg\Delta^{-1}} b_1 + (t_s-a)G_{\mathrm{S}} \tag{17}$$

by fitting b_1 and G_{S} to $S(t_s)$. We have extended the number of source-sink separations compared to our analysis of the isovector vector form factor [54] to include smaller source-sink separations. This enables us to monitor the range of t_s where the result from the linear ansatz of Eq. (17) stabilizes.

Rather than selecting a single fit starting at a certain value t_s^{min}, we follow the procedure defined in [55] and determine G_S from an average over a range of t_s^{min} values with weights

$$w(t_s^{\mathrm{min}}) = \frac{1}{2\mathcal{N}}\left[\tanh\frac{t_s^{\mathrm{min}}-t_{\mathrm{lo}}}{\Delta t} - \tanh\frac{t_s^{\mathrm{min}}-t_{\mathrm{up}}}{\Delta t}\right], \tag{18}$$

with $\mathcal{N}$ a normalization factor. The choice of lower (t_{lo}) and upper (t_{up}) bound suppresses the excessive influence of excited states at small values of t_s and the exponentially increasing noise at larger values, respectively. We find the choices

$$t_{\mathrm{lo}} = 0.8\ \mathrm{fm}, \quad t_{\mathrm{up}} = 1.0\ \mathrm{fm}, \quad \text{and} \quad \Delta t = 0.08\ \mathrm{fm}, \tag{19}$$

to give estimates for the ground-state matrix element that are more robust against statistical fluctuations than choosing one particular value of t_s^{min}. Since the onset of a plateau in the extracted matrix element as a function of t_s^{min}, such as in the left panel of Fig. 1, does not entirely exclude the possibility of remnant excited-state contributions, we also apply two further analysis methods. We note that the average using Eq. (18) is only applied to the fit results of Eq. (17) for different t_s^{min}.

As a cross check, we performed fits to the summed correlator including the first excited-state contribution,

$$S(t_s) = \tilde{b}_1 + (G_{\mathrm{S}} + \tilde{m}_{11}e^{-t_s\Delta})t_s + \frac{2\tilde{m}_{10}}{\sinh(a\Delta/2)}e^{-t_s\Delta/2}\sinh\frac{(t_s-a)\Delta}{2} + \ldots \tag{20}$$

where $\tilde{m}_{10}$ and $\tilde{m}_{11}$ involve matrix elements of S_q from first excited to ground state and excited to excited state, respectively. The excited-state contributions are parametrically suppressed by $\Delta\cdot t_s$. In this case, we need priors for

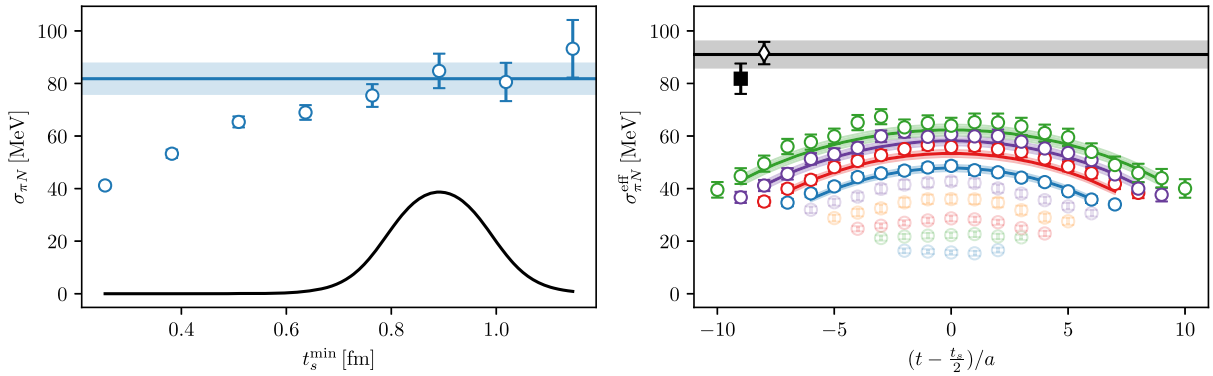

FIG. 1. Left: Results of linear fits to the summed correlator on ensemble D200 with the starting time slice given on the x-axis. The blue shaded area is the weighted average using Eq. (18) shown as a black line in the bottom of the plot, for the particular choice of parameters from Eq. (19). Right: fit result of an explicit two-state fit to the effective form factor. The gray band represents the result for the ground-state matrix element of that fit; it is shown together with the result of the window average (black filled square) and the result of a two-state fit to the summed correlator (black diamond).

the energy gap Δ in order to stabilize the fits. We choose twice the pion mass on the given ensemble as the central value and assign a total prior width of 5%. Even with a prior for the energy gap Δ, $\tilde{m}_{11}$ is not well constrained, and we resort to a simplified fit ansatz excluding this term.

In addition to the analysis of the summed correlators, we performed fits using a two-state ansatz for the effective form factor itself. The fit function reads

$$G_S^{\mathrm{eff}}(t,t_s) = G_S + m_{10}\exp\left[-\Delta t\right] + m_{10}\exp\left[-\Delta(t_s-t)\right] + m_{11}\exp\left[-\Delta t_s\right]. \quad (21)$$

Similar to the analysis of the summed correlators, the gap of the first excited state is not well constrained, and we are led to using priors. For the priors, we use the same setup as in the two-state fit to the summed correlator. Even though the neglected excited-state contributions in the two-state ansatz are parametrically less suppressed, we include all $t_s > 0.8$ fm, i.e., the same value as for t_{lo} in Eq. (19). Subsequently, we cut time slices at the source and sink until a good fit is achieved. For σ_s the data is too noisy to perform two-state fits of the effective form factor, and we resort to plateau fits, where we fit different t_s and use the value that shows convergence with t_s. A two-state fit applied to data at $m_\pi = 200$ MeV is illustrated in Fig. 1 (right panel), along with the results of the two other methods. Figure 2 shows a comparison of the σ terms obtained from the different excited-state analyses, and the results are collected in Table III in the Supplemental Material [56].

While the summation method with the averaging window fixed in units of fm is adequate if the dominant excited-state contribution is only weakly dependent on the pion mass, the two other analysis methods explicitly assume the bulk of that contribution to be associated with a mass gap $\Delta = \mathrm{O}(m_\pi)$. Therefore, in terms of excited-state contamination, we essentially have two procedures, either relying on the applicability of Eq. (17) or, relying on assumptions about the energy gaps through priors, applying Eqs. (20) and (21), where the latter are both very sensitive to the prior, but give consistent results. In order to assess the systematics associated with the very different effects of excited states in the two strategies, we perform the chiral and continuum extrapolation for the window averaged summation method [fit ansatz Eq. (17)] and for one method using priors [fit ansatz Eq. (21)], and finally model average the results with equal weights, i.e., giving no preference to either strategy.

Chiral and continuum extrapolation.—The calculation of the σ term in chiral perturbation theory (ChPT) proceeds via the nucleon mass using the Feynman-Hellmann theorem. The nucleon mass has been calculated in various formulations of ChPT [27,64–66] up to two-loop order [67].

Since our gauge ensembles lie on a line of constant trace of the quark mass matrix $(2m_l + m_s)$, both the pion and the kaon mass change as m_l is varied. Moreover, to have a handle on the quantities σ_0 and σ_s, the inclusion of the strange quark into the effective theory is mandatory. We therefore use the result of SU(3) ChPT in the extended on-mass shell scheme of [68]. The nucleon mass reads

$$m_N = m_0 - \underbrace{(2b_0 + 4b_f)}_{\hat{b}_0} M_\pi^2 - \underbrace{(4b_0 + 4b_d - 4b_f)}_{\hat{b}_1} M_K^2 + \mathcal{F}_\pi I_{MB}(M_\pi) + \mathcal{F}_K I_{MB}(M_K) + \mathcal{F}_\eta I_{MB}(M_\eta), \quad (22)$$

with

$$\mathcal{F}_\pi = -\frac{3}{4}\left(D^2 + 2DF + F^2\right), \quad (23)$$

$$\mathcal{F}_K = -\left(\frac{5}{6}D^2 - DF + \frac{3}{2}F^2\right), \quad (24)$$

$$\mathcal{F}_\eta = -\frac{1}{2}\left(\frac{1}{6}D^2 - DF + \frac{3}{2}F^2\right), \quad (25)$$

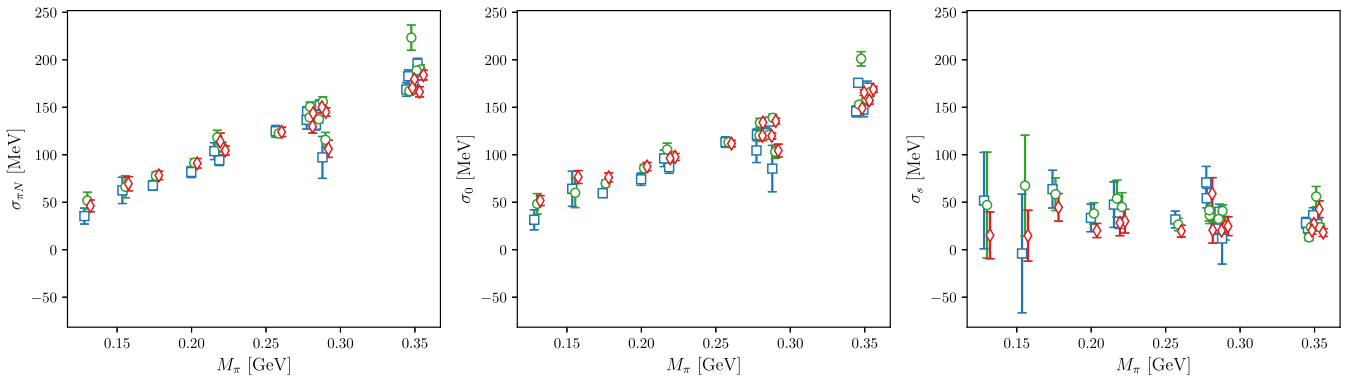

FIG. 2. Comparison of the different extractions. The blue squares, green circles, and red diamonds correspond to the extraction based on the window average of the summed correlator, the explicit two-state fit to the summed correlator, and the explicit two-state fit to the effective form factor.

$$I_{MB}(M) = \frac{M^3}{8F_\phi^2 m_0 \pi^2}\left(M\log\frac{M}{m_0} + \sqrt{4-\frac{M^2}{m_0^2}}m_0 \arccos\left(\frac{M}{2m_0}\right)\right). \quad (26)$$

For the η meson mass, we assume the Gell-Mann-Okubo relation $3M_\eta^2 = 4M_K^2 - M_\pi^2$. We fix the values of the low-energy constants $D = 0.8$, $F = 0.46$, $F_\phi = 0.108$ GeV, $m_0 = 938.9$ MeV and fit the constants $\hat{b}_0$ and $\hat{b}_1$. For the physical point we use the isospin-limit meson masses $M_\pi = 134.8$ MeV and $M_K = 494.2$ MeV [69]. Equation (22) is derived with respect to the quark masses, yielding the quark-mass dependence of the sigma terms. For the quark-mass dependence of the octet meson masses we take the leading order expression in ChPT [70].

We treat the lattice spacing dependence of the sigma term via an additional term [71],

$$\sigma_{\pi N/s} \to \sigma_{\pi N/s} + b_i \frac{a}{\sqrt{t_0}} M_{\pi/K}^2. \quad (27)$$

The finite-volume dependence of the nucleon mass in SU(2) is given in [72], from which we derive

$$\sigma_{\pi N} \to \sigma_{\pi N} + b_L\left(\frac{M_\pi^3}{M_\pi L} - \frac{M_\pi^3}{2}\right)\exp\left(-M_\pi L\right). \quad (28)$$

We only use the finite-volume corrections due to pion loops, as terms $\sim\exp(-M_K L)$ are parametrically much more suppressed; thus we omit finite-volume corrections for σ_s. Instead of using the ChPT results for the prefactors of the finite-volume corrections, we leave them as additional fit parameters; however we use as a loose prior the value obtained from SU(2) ChPT.

We proceed to fit $\sigma_{\pi N}$, σ_s, taking into account the correlations among the sigma terms and lattice spacing. The fits are performed with variations in the upper end of the pion mass range (220, 285, or 360 MeV), and including/excluding the artifacts with respect to finite lattice spacing and to finite volume. We analyze the two datasets obtained from the excited-state analyses separately with respect to the above variations, i.e., within each dataset all variations are averaged using an AIC weight w_i given by

$$w_i = a_i / \left(\sum_k a_k\right), \quad a_i = \exp -\frac{1}{2}\left[\chi^2 + 2n_c + 2n_f\right], \quad (29)$$

where n_c and n_f denote the number of cut data points and number of fit parameters, respectively. The weights are normalized per dataset, and finally a flat weighting is applied between the datasets. Using the procedure of [54,73] we obtain as our final estimates

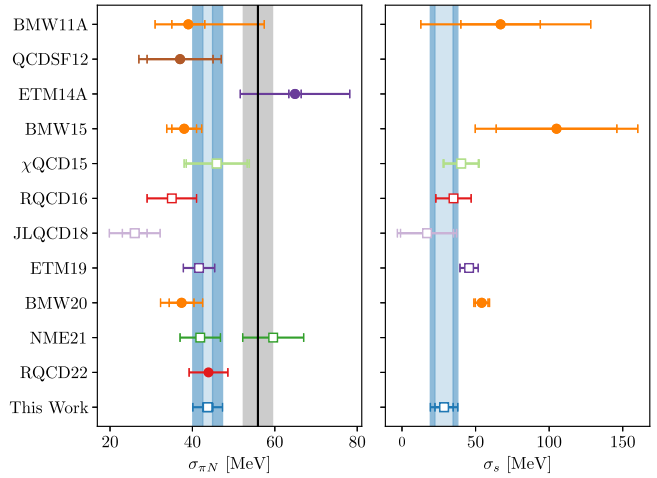

FIG. 3. Comparison of our results to other lattice determinations: RQCD22 [20], NME21 [26], BMW20 [19], ETM19 [18], JLQCD18 [17], RQCD16 [16], χQCD15 [15], BMW15 [14], ETM14A [13], QCDSF12 [10], and BMW11A [9]. Filled circles represent results extracted from the slope of the nucleon mass with respect to the light quark mass m_l, and squares represent results obtained directly from the matrix element. The gray band corresponds to the dispersive result of [5] with the correction for the isospin-limit value of the pion mass from [74] applied, i.e., $\sigma_{\pi N} = 55.9(3.5)$ MeV.

$$\sigma_{\pi N} = 43.7(1.2)(3.4)\ \text{MeV} \quad (30a)$$

$$\sigma_0 = 41.3(1.2)(3.4)\ \text{MeV} \quad (30b)$$

$$\sigma_s = 28.6(6.2)(7.0)\ \text{MeV}, \quad (30c)$$

where the first and second errors correspond to the statistical and systematic uncertainties, respectively. More details of the averaging procedure are given in the Supplemental Material [56]. The systematic error dominates, with the largest source of uncertainty coming from the treatment of excited states. In Fig. 3 we compare our results to those of other lattice calculations. We note a reasonable agreement among these calculations.

Conclusion.—We have calculated the nucleon sigma terms $\sigma_{\pi N}$, σ_0, and σ_s with a full error budget concerning excited-state contamination as well as chiral, finite-size, and continuum extrapolations. Our estimate for $\sigma_{\pi N}$ lies close to the early estimate from $N\pi$ scattering [4]. It is compatible with most other lattice determinations and in excellent agreement with the $\sigma_{\pi N}$ determination of [20], which uses an overlapping set of gauge ensembles but proceeds by computing the quark-mass dependence of the nucleon mass. For σ_s we find a nonzero value, again compatible with most recent lattice determinations. Including the effects of different methods for the treatment

TABLE II. Result of the model average procedure using AIC weights defined in Eq. (29) when applied exclusively to the dataset denoted in the column heading. Only total errors are shown.

i:	Window	Two-state
$\sigma^i_{\pi N}$	42.3(2.4) MeV	46.9(1.7) MeV
σ^i_s	39.6(1.9) MeV	45.0(1.7) MeV
σ^i_0	34.2(9.8) MeV	24.7(6.5) MeV

of excited states into our error budget, we clearly establish this to be the largest source of systematic uncertainty. Analyzing the datasets from the window and two-state procedure separately (see Table II), we observe an upward trend for $\sigma_{\pi N}$ when using priors similar to [26], albeit not as pronounced. Our final central value for $\sigma_{\pi N}$ lies between the two values presented in [26], but is much closer to that obtained without imposing tight priors on the gap Δ around values of order m_π. A discrepancy of 2.4σ persists with the dispersive result of [5], after applying the correction necessary to match our definition of the pion mass in the isospin limit from Ref. [74].

We thank Marco Cè for sharing his values of the PCAC masses calculated in the context of [46], and Simon Kuberski for providing improved reweighting factors [75] for the gauge ensembles used in our calculation. This work was supported in part by the European Research Council (ERC) under the European Unions Horizon 2020 research and innovation program through Grant Agreement No. 771971-SIMDAMA and by the Deutsche Forschungsgemeinschaft (DFG) under Grant No. HI 2048/1-2 (Project No. 399400745) and in the Cluster of Excellence Precision Physics, Fundamental Interactions and Structure of Matter (PRISMA + EXC 2118/1), funded by the DFG within the German Excellence strategy (Project ID No. 39083149). Calculations for this project were partly performed on the HPC clusters "Clover" and "HIMster2" at the Helmholtz Institute Mainz, and "Mogon 2" at Johannes Gutenberg- Universität Mainz. The authors gratefully acknowledge the Gauss Centre for Supercomputing e.V. [76] for funding this project by providing computing time on the GCS Supercomputer systems JUQUEEN and JUWELS at Jülich Supercomputing Centre (JSC) via Grants No. NucStrucLFL, No. HMZ21, No. HMZ23, and No. HMZ36 [the latter through the John von Neumann Institute for Computing (NIC)], as well as on the GCS Supercomputer HAZELHEN at Höchstleistungsrechenzentrum Stuttgart [77] under Project No. GCS-HQCD. Our programs use the QDP++ library [78] and deflated SAP + GCR solver from the openQCD package [79], while the contractions have been explicitly checked using [80]. We are grateful to our colleagues in the CLS initiative for sharing the gauge field configurations on which this work is based.

[1] G. Jungman, M. Kamionkowski, and K. Griest, Phys. Rep. **267**, 195 (1996).
[2] We take the nucleon at rest and use the state normalization $\langle N\vec{p}'s'|N\vec{p}s\rangle = (2\pi)^3\delta^{ss'}\delta(\vec{p}-\vec{p}')$. Also, throughout this Letter we assume exact isospin symmetry.
[3] T. P. Cheng and R. F. Dashen, Phys. Rev. Lett. **26**, 594 (1971).
[4] J. Gasser, H. Leutwyler, and M. E. Sainio, Phys. Lett. B **253**, 252 (1991).
[5] M. Hoferichter, J. Ruiz de Elvira, B. Kubis, and U.-G. Meißner, Phys. Rev. Lett. **115**, 092301 (2015).
[6] J. M. Alarcon, J. Martin Camalich, and J. A. Oller, Phys. Rev. D **85**, 051503(R) (2012).
[7] J. Ruiz de Elvira, M. Hoferichter, B. Kubis, and U.-G. Meißner, J. Phys. G **45**, 024001 (2018).
[8] M. Hoferichter, J. Ruiz de Elvira, B. Kubis, and U.-G. Meißner, Phys. Rep. **625**, 1 (2016).
[9] S. Dürr *et al.*, Phys. Rev. D **85**, 014509 (2012); **93**, 039905 (E) (2016).
[10] G. S. Bali *et al.*, Nucl. Phys. **B866**, 1 (2013).
[11] P. E. Shanahan, A. W. Thomas, and R. D. Young, Phys. Rev. D **87**, 074503 (2013).
[12] M. Engelhardt, Phys. Rev. D **86**, 114510 (2012).
[13] C. Alexandrou, V. Drach, K. Jansen, C. Kallidonis, and G. Koutsou, Phys. Rev. D **90**, 074501 (2014).
[14] S. Dürr *et al.*, Phys. Rev. Lett. **116**, 172001 (2016).
[15] Y.-B. Yang, A. Alexandru, T. Draper, J. Liang, and K.-F. Liu (xQCD), Phys. Rev. D **94**, 054503 (2016).
[16] G. S. Bali, S. Collins, D. Richtmann, A. Schäfer, W. Söldner, and A. Sternbeck (RQCD Collaboration), Phys. Rev. D **93**, 094504 (2016).
[17] N. Yamanaka, S. Hashimoto, T. Kaneko, and H. Ohki (JLQCD Collaboration), Phys. Rev. D **98**, 054516 (2018).
[18] C. Alexandrou, S. Bacchio, M. Constantinou, J. Finkenrath, K. Hadjiyiannakou, K. Jansen, G. Koutsou, and A. Vaquero Aviles-Casco, Phys. Rev. D **102**, 054517 (2020).
[19] S. Borsanyi, Z. Fodor, C. Hoelbling, L. Lellouch, K. K. Szabo, C. Torrero, and L. Varnhorst (2020), arXiv:2007.03319.
[20] G. S. Bali, S. Collins, P. Georg, D. Jenkins, P. Korcyl, A. Schäfer, E. E. Scholz, J. Simeth, W. Söldner, and S. Weishäupl (RQCD Collaboration), J. High Energy Phys. 05 (2023) 035.
[21] Y. Aoki *et al.* (Flavour Lattice Averaging Group (FLAG)), Eur. Phys. J. C **82**, 869 (2022).
[22] L. Alvarez-Ruso, T. Ledwig, J. Martin Camalich, and M. J. Vicente-Vacas, Phys. Rev. D **88**, 054507 (2013).
[23] X.-L. Ren, X.-Z. Ling, and L.-S. Geng, Phys. Lett. B **783**, 7 (2018).
[24] M. F. M. Lutz, Y. Heo, and X.-Y. Guo, Nucl. Phys. **A977**, 146 (2018).
[25] M. F. M. Lutz, Y. Heo, and X.-Y. Guo, Eur. Phys. J. C **83**, 440 (2023).
[26] R. Gupta, S. Park, M. Hoferichter, E. Mereghetti, B. Yoon, and T. Bhattacharya, Phys. Rev. Lett. **127**, 242002 (2021).
[27] J. M. Alarcon, L. S. Geng, J. Martin Camalich, and J. A. Oller, Phys. Lett. B **730**, 342 (2014).
[28] H. Akaike, B. N. Petrov, and F. Csaki, in *Proceedings of the Second International Symposium on Information Theory* (Akadémiai Kiadó, Budapest, 1973).

[29] H. Akaike, IEEE Trans. Autom. Control **19**, 716 (1974).
[30] M. Bruno *et al.*, J. High Energy Phys. 02 (2015) 043.
[31] B. Sheikholeslami and R. Wohlert, Nucl. Phys. **B259**, 572 (1985).
[32] M. Lüscher and P. Weisz, Commun. Math. Phys. **97**, 59 (1985); **98**, 433(E) (1985).
[33] D. Mohler and S. Schaefer, Phys. Rev. D **102**, 074506 (2020).
[34] M. Cè *et al.*, Phys. Rev. D **106**, 114502 (2022).
[35] M. Bruno, T. Korzec, and S. Schaefer, Phys. Rev. D **95**, 074504 (2017).
[36] S. Güsken, U. Löw, K. H. Mütter, R. Sommer, A. Patel, and K. Schilling, Phys. Lett. B **227**, 266 (1989).
[37] M. Albanese *et al.* (APE Collaboration), Phys. Lett. B **192**, 163 (1987).
[38] G. Martinelli and C. T. Sachrajda, Nucl. Phys. **B316**, 355 (1989).
[39] G. S. Bali, S. Collins, and A. Schafer, Comput. Phys. Commun. **181**, 1570 (2010).
[40] T. Blum, T. Izubuchi, and E. Shintani, Phys. Rev. D **88**, 094503 (2013).
[41] E. Shintani, R. Arthur, T. Blum, T. Izubuchi, C. Jung, and C. Lehner, Phys. Rev. D **91**, 114511 (2015).
[42] L. Giusti, T. Harris, A. Nada, and S. Schaefer, Eur. Phys. J. C **79**, 586 (2019).
[43] C. McNeile and C. Michael (UKQCD), Phys. Rev. D **73**, 074506 (2006).
[44] V. Gülpers, G. von Hippel, and H. Wittig, Phys. Rev. D **89**, 094503 (2014).
[45] A. Stathopoulos, J. Laeuchli, and K. Orginos, SIAM J. Sci. Comput. **35**, S299 (2013).
[46] M. Cè, A. Gérardin, G. von Hippel, H. B. Meyer, K. Miura, K. Ottnad, A. Risch, T. San José, J. Wilhelm, and H. Wittig, J. High Energy Phys. 08 (2022) 220.
[47] G. Parisi, Phys. Rep. **103**, 203 (1984).
[48] G. P. Lepage, in *From actions to answers. Proceedings, Theoretical Advanced Study Institute in Elementary-particle Physics (TASI '89)*, edited by T. A. DeGrand and D. Toussaint (World Scientific, Singapore, 1989).
[49] K. Ottnad, Eur. Phys. J. A **57**, 50 (2021).
[50] D. Djukanovic, Proc. Sci., LATTICE2021 (**2022**) 009 [arXiv:2112.00128].
[51] L. Maiani, G. Martinelli, M. L. Paciello, and B. Taglienti, Nucl. Phys. **B293**, 420 (1987).
[52] S. J. Dong, K. F. Liu, and A. G. Williams, Phys. Rev. D **58**, 074504 (1998).
[53] S. Capitani, M. Della Morte, G. von Hippel, B. Jäger, A. Jüttner, B. Knippschild, H. B. Meyer, and H. Wittig, Phys. Rev. D **86**, 074502 (2012).
[54] D. Djukanovic, T. Harris, G. von Hippel, P. M. Junnarkar, H. B. Meyer, D. Mohler, K. Ottnad, T. Schulz, J. Wilhelm, and H. Wittig, Phys. Rev. D **103**, 094522 (2021).
[55] D. Djukanovic, G. von Hippel, J. Koponen, H. B. Meyer, K. Ottnad, T. Schulz, and H. Wittig, Phys. Rev. D **106**, 074503 (2022).
[56] See Supplemental Material at http://link.aps.org/supplemental/10.1103/PhysRevLett.131.261902, which includes Refs. [56–62].
[57] T. Bhattacharya, R. Gupta, W. Lee, S. R. Sharpe, and J. M. S. Wu, Phys. Rev. D **73**, 034504 (2006).
[58] A. Gérardin, T. Harris, and H. B. Meyer, Phys. Rev. D **99**, 014519 (2019).
[59] P. Korcyl and G. S. Bali, Phys. Rev. D **95**, 014505 (2017).
[60] S. Sint and R. Sommer, Nucl. Phys. **B465**, 71 (1996).
[61] X.-D. Ji, Phys. Rev. Lett. **74**, 1071 (1995).
[62] K. Takeda, S. Aoki, S. Hashimoto, T. Kaneko, J. Noaki, and T. Onogi, Phys. Rev. D **83**, 114506 (2011).
[63] E. T. Neil and J. W. Sitison, Phys. Rev. E **108**, 045308 (2023).
[64] B. Borasoy and U.-G. Meissner, Ann. Phys. (N.Y.) **254**, 192 (1997).
[65] X. L. Ren, L. S. Geng, J. Martin Camalich, J. Meng, and H. Toki, J. High Energy Phys. 12 (2012) 073.
[66] D. Severt, U.-G. Meißner, and J. Gegelia, J. High Energy Phys. 03 (2019) 202.
[67] M. R. Schindler, D. Djukanovic, J. Gegelia, and S. Scherer, Phys. Lett. B **649**, 390 (2007).
[68] B. C. Lehnhart, J. Gegelia, and S. Scherer, J. Phys. G **31**, 89 (2005).
[69] S. Aoki *et al.*, Eur. Phys. J. C **77**, 112 (2017).
[70] J. Gasser and H. Leutwyler, Nucl. Phys. **B250**, 465 (1985).
[71] Note that the current is not $\mathcal{O}(a)$ improved.
[72] S. R. Beane, Phys. Rev. D **70**, 034507 (2004).
[73] S. Borsanyi *et al.*, Nature (London) **593**, 51 (2021).
[74] M. Hoferichter, J. R. de Elvira, B. Kubis, and U.-G. Meißner, Phys. Lett. B **843**, 138001 (2023).
[75] S. Kuberski, arXiv:2306.02385.
[76] www.gauss-centre.eu
[77] www.hlrs.de
[78] R. G. Edwards and B. Joo (SciDAC, LHPC, and UKQCD Collaborations), Nucl. Phys. B, Proc. Suppl. **140**, 832 (2005).
[79] M. Lüscher and S. Schaefer, Comput. Phys. Commun. **184**, 519 (2013).
[80] D. Djukanovic, Comput. Phys. Commun. **247**, 106950 (2020).